SINGLE MICROHOLE per PIXEL in CMOS IMAGE SENSORS with ENHANCED OPTICAL SENSITIVITY in NEAR-INFRARED

E.Ponizovskaya Devine[1,2,*], *Senior Member, IEEE*, Wayesh Qarony[2], Ahasan Ahamed[2], *Member, IEEE*, Ahmed S. Mayet[2], *Member, IEEE*, Soroush Ghandiparsi[2], *Member, IEEE*, Cesar Bartolo-Perez[2], *Member, IEEE*, Aly F Elrefaie[1], *Life Fellow, IEEE*, Toshishige Yamada[1,3], *Senior Member, IEEE*, Shih-Yuan Wang[1], *Life Fellow, IEEE,* M Saif Islam[2,*], *Fellow, IEEE*

Abstract— Silicon photodiode-based CMOS sensors with backside-illumination for 300–1100 nm wavelength range were studied. We showed that a single hole in the photodiode increases the optical efficiency of the pixel. In near-infrared wavelengths, the enhancement allows 70% absorption in a 3 μm thick Si. It is 4x better than that for the flat pixel. We compared different shapes and sizes of single hole and hole arrays. We have shown that a certain size and shape in single hole-based pixels contribute to stronger enhancement of optical efficiencies. The crosstalk was successfully reduced by employing trenches between pixels. We optimized the dimensions of the trenches to achieve minimal pixel separation for 1.12 μm pixels.

Index Terms—CMOS image sensors, photon-trapping, high-efficiency sensors

I. INTRODUCTION

THE interests in the complementary metal-oxide-semiconductor (CMOS) image sensors are increasing due to the growing demand for mobile imaging, digital cameras, surveillance, monitoring, and biometrics. Image sensors have been adopted in a significant number of products [1][2][3] and have a multitude of applications. One such application is night-time surveillance and monitoring, which demand high sensitivity as well as improved resolution in the near-infrared wavelength spectrum. Several manufacturing companies are competing with each other to bring a higher resolution imager to the market. This constant drive to increase the pixel density has resulted in a 2.5-fold reduction in the pixel pitch from 2.2 μm (Micron-2006) to even 0.8 μm (Sony-2019) over the past decade [4]. The trade-off for such improvement came in the form of loss in optical sensitivity due to the reduction of the absorption area. This can be resolved by using a thicker absorbing layer. However, the thicker absorber layer reduces the speed of operation, thus affecting the bandwidth of the imager. To mitigate this trade-off between resolution-efficiency-speed, we investigate the use of microholes enhancing the optical efficiency of the imagers in the near-infrared wavelength region [5][6]. We observe an enhanced optical efficiency in the near-infrared spectrum compared to the same structure without the microholes. In general, CMOS image sensors can have pixel sizes of 2 μm × 2 μm or even smaller dimensions [7]. CMOS sensors having such small pixel sizes contribute to a major challenge in suppressing the

parasitic charge exchanges between neighboring pixels (crosstalk). Although the insertion of microhole arrays increases the crosstalk between pixels, it was reduced using the deep trench isolation (DTI) [8][9].
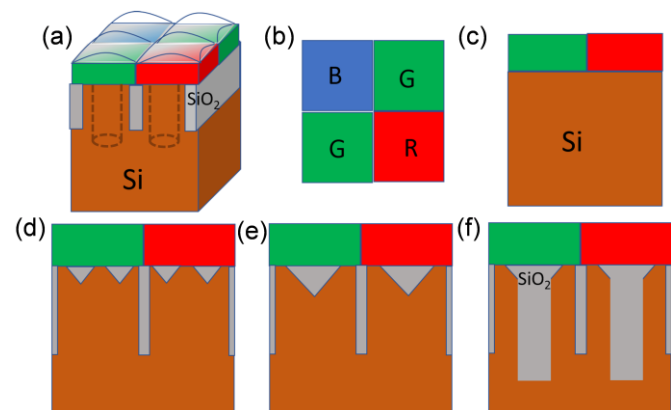

Fig. 1. Schematic diagram of CMOS image pixels: a) view of the pixel with micro lenses, color filters, and trenches; b) Bayer filter array c) planar pixel with color filters d) pixels with inverted pyramids array; e) pixel with a single inverted pyramid, and d) pixel with single funnel holes.

We are considering a stacked structure similar to the one reported by Sony that exhibited low noise [10], were back-side illuminated and layered over a chip where signal processing circuits are formed. One advantage of this configuration is that large-scale circuits can be mounted on a relatively small chip. Since each section is formed on a separate chip, specialized manufacturing processes can be used to produce high performance imaging sensors and a state-of-the-art circuit section, enabling higher resolution, multi functionality, and a

[1] W&WSens Device, 4546 El Camino, Los Altos, CA 94022 USA
[2] University of California, Davis, CA 95616 USA
[3] University of California, Santa Cruz, Santa Cruz, CA 95064 USA
*Contact emails: eponizovskayadevine@ucdavis.edu, sislam@ucdavis.edu

compact size. Besides chip size, the stacking technology improves dark characteristics, such as noise and white pixels, by optimizing the sensor process independently.

Two different methods are implemented for near-infrared imaging: (i) application of a separate near-infrared filter, based on plasmonic techniques [11], or gratings [12]; and (ii) standard low-cost pigment filters [13] that are transparent in near-infrared wavelengths. Infrared images are reconstructed based on the techniques discussed in Ref. [14]. To increase the quantum efficiency, the surface of the pixels is etched with an array of small inverted pyramids with dimensions in the range of 400 nm [3]. We model a Bayer array with a commonly used color filter array [15].

We discuss the different approaches to increase the optical efficiency in infrared wavelengths. It was shown [5] that the microholes arrays can drastically increase the optical efficiency of Si in 800-1000 nm wavelength range. Here, we propose to use a single hole per diode. The hole size is in the range of 800-1000 nm. We simulated CMOS image sensors with different hole shapes, such as a pyramid, cylindrical, and funnel shapes [6], and we compared the optical efficiency and the crosstalk for each shape. The deep trench structure [8][9] with Si-SiO$_2$ interface is used as a barrier against electron diffusion. This also helps in confining light within the pixels by acting as a reflector between pixels. We simulated 1.12 μm wide and 3 μm deep pixels with trenches of 0 to 250 nm width and 0 to 2.9 μm depth. Our simulations show that a single funnel hole in a device provides better efficiency compared to an array. A funnel-shaped hole with a size comparable to the wavelength converts propagation direction of light into lateral, and provides better light trapping effect and reduces the reflection, as was shown in Ref [16][17][18] that implemented this technique for high-speed Si photodetectors. The same shape single holes were used for the simulations. We used the Lumerical FDTD software and the methodology of the simulation that was described in [1] to calculate the absorption
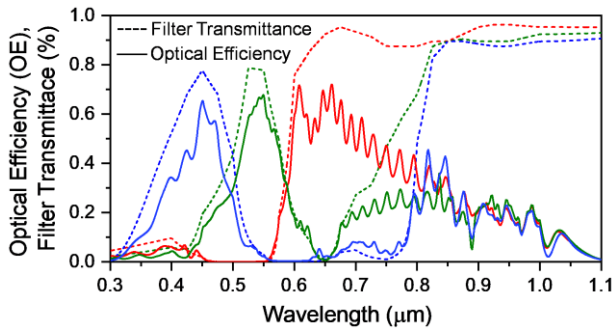

Fig. 2. Simulated transmittance after filters (dashed lines) and optical efficiency (OE) of a flat pixel without DTI (solid lines).

in each pixel. The single funnel hole enhanced the absorption by more than 60% at 850 nm and 940 nm wavelength for pixel of 1.12×1.12 μm lateral dimension and 3 μm depth. This is two times thinner than the devices reported in [1] and significantly exceeds the results reported in [2][3] for inverted pyramids arrays.

II. OPTICAL SIMULATION METHODOLOGY

It was demonstrated in Ref. [5] that the microstructure morph, the surface illuminating light into lateral directions parallel to the plane of the surface where it is absorbed while the generated electro-hole pairs are collected through the intrinsic Si layer. An effective light trapping can be observed in a slab of Si, if there are modes that stay in the slab with the wave vector almost parallel to the interface. The modes can be guided resonance modes that stay in the structure until they are absorbed. Alternatively, they could be leaky modes that could be useful if they are absorbed before they leak out. If some of these modes correspond to slow light, they contribute to increased absorption in Si. Successful conversion of an initial incident vertical plane waves to an ensemble of lateral collective modes can be realized in a 2D periodic array of
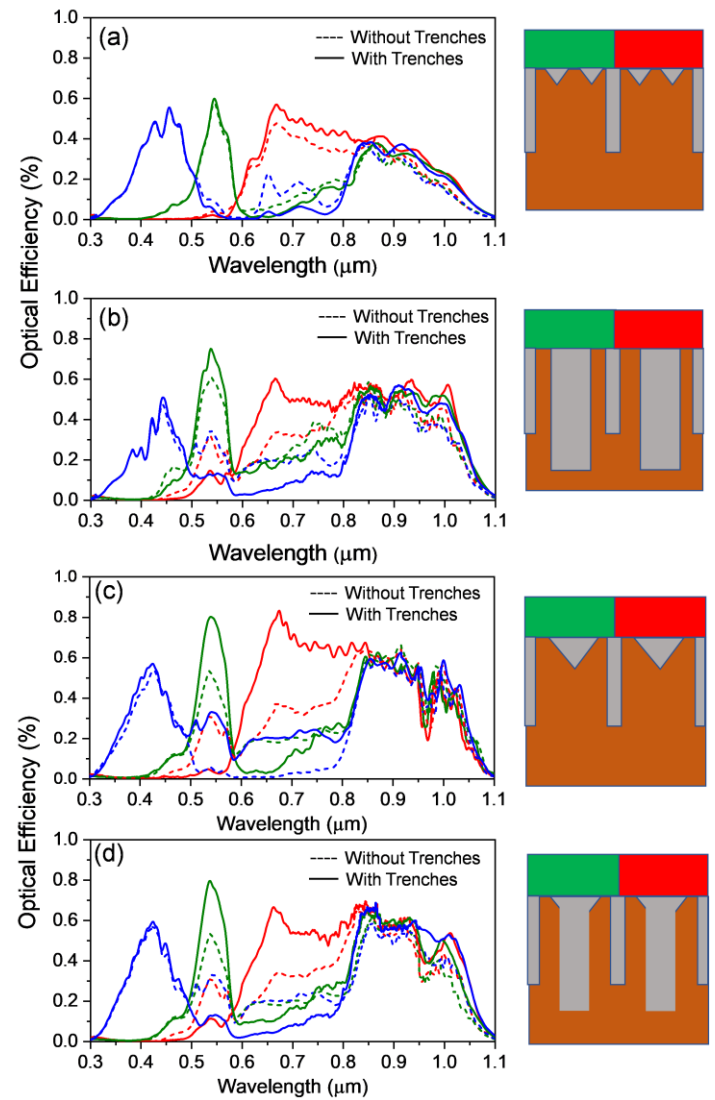

Fig. 3. Calculated optical efficiency (OE) with (solid) and without (dashed) trenches for (a) inverted pyramids array, (b) single cylindrical holes, (c) single inverted pyramid, and (d) single funnel shaped hole.

holes.

We used a Finite Difference Time Domain (FDTD) [19] Lumerical tool [20] to solve Maxwell's curl equations for the unit cell of Bayer array (Fig. 1), where Bloch boundary conditions around the cell and Perfectly Matched Layer (PML) in the direction normal to the surface were considered. First, we found that a single hole can couple light into the parallel-to-the-interface modes. Next, we analyzed the array of

TABLE I

CROSSTALK INDEX (INTENSITY OF PIXEL/INTENSITY FROM SIDE PIXEL) OF THE SIMULATED IMAGE SENSORS INTEGRATED WITH PHOTON-TRAPPING HOLES WITH INVERTED PYRAMIDS ARRAY, SINGLE CYLINDRICAL PYRAMID, SINGLE CYLINDRICAL HOLE, AND SINGLE FUNNEL HOLE, WHERE A FLAT PIXEL IS SIMULATED AS A REFERENCE. HIGHER CROSSTALK INDEX INDICATES LOWER CROSSTALK.

Holes Design/Structure	Pixel Color	Crosstalk index No DTI/DTI	OE (%) @ 850/940nm
Flat pixels	Red-green	4	22/15
	Red-blue	26	
	Green- Red	20	
	Green-Blue	7.5	
	Blue-Red	24	
	Blue-Green	2.97	
Inverted pyramids Array	Red-green	6.1/26	35/20
	Red-blue	2.6/17.9	
	Green- Red	13.5/30	
	Green-Blue	6.8/14	
	Blue-Red	24/24	
	Blue-Green	9.97/30	
Single Inverted Pyramid	Red-green	1.6/14.7	60/52
	Red-blue	4.8/63	
	Green- Red	2.8/20	
	Green-Blue	2.5/17.3	
	Blue-Red	50/24	
	Blue-Green	6.2/130	
Single Cylindrical hole	Red-green	1.5/2.9	58/50
	Red-blue	1.2/10.9	
	Green- Red	2.1/5.6	
	Green-Blue	1.9/5.5	
	Blue-Red	76/26	
	Blue-Green	6/63	
Single Funnel hole	Red-green	1.34/6.9	71/55
	Red-blue	1.3/19.9	
	Green- Red	1.68/7.9	
	Green-Blue	1.48/7.7	
	Blue-Red	21/24	
	Blue-Green	5.5/30	

the holes and coupling of the parallel to the interface modes into the guided resonant modes or into the leaky modes and

theoretically calculate the increase in absorption. The hole parameter optimization was done based on the theoretical calculation.

CMOS image sensor model includes lenses, red, green, and blue filters with a thickness of 900 nm, antireflection coating, and a 3 μm thick Si on a SOI substrate. A micro-lens with a radius and thickness of 1 μm and 500 nm was also assumed on the top of each sensor. Additionally, different shapes and sizes of holes were considered as photon-trapping structures to enhance the absorption efficiency or optical efficiency of the sensors, where trenches filled with silicon oxide were assumed. Herein, we compared several designs: flat pixel with no surface photon-trapping structure (Fig.1c), an array of holes with 400 × 400 nm inverted pyramids [3] (Fig.1d), pixel with a single inverted pyramid of 900 × 900 nm (Fig1.e), a funnel hole with a diameter of 900 nm and an angle of 60 degree wall that merges with 800 nm diameter and 2 μm deep cylindrical hole (Fig. 1f), and a cylindrical hole with a diameter and depth of 800 nm and 2 μm, respectively. A plane wave source was considered with normal incidence to the surface for the wavelengths ranging between 300 and 1100 nm.

The Poynting vector (P) was measured around the cells. For a given current J in the pixel and electric field, E, the energy absorbed in volume V is calculated by applying the divergence theorem for stable state as below:

$$\int_V \frac{1}{2}\mathrm{Re}\left(E \cdot J^*\right)\cdot dv = \int_V \frac{1}{2}\nabla \cdot \mathrm{Re}\left(E \times H^*\right)\cdot dv$$
$$= -\oint_S \frac{1}{2}\left[\mathrm{Re}\left(E \times H^*\right)\cdot \vec{n}\right]ds \qquad (1)$$

where, S is the surface that surrounds the volume V and $\vec{n}$ is the unit vector normal to the surface S. Thus, to calculate the optical absorption in each pixel power, we integrate the Poynting vector normal to the surface over the surface of the depletion region of the pixel. The results present the difference between the real parts of the Poynting flux entering the volume at the surface between the filters and the pixel ($P_{in} = \mathrm{Re}\left(E \times H^*\right)$), and the Poynting flux leaving the pixel (P_{out}), that are simulated with FDTD method.

The optical efficiency is calculated as following:

$$OE = \frac{P_{in} - P_{out}}{P_{inc}} \qquad (2)$$

where, P_{inc} is the Poynting vector of the incident light calculated above the lenses and filters. In this study, it is assumed that the quantum efficiency is proportional to the optical efficiency [21]. It should be noted that the calculated optical efficiencies are not normalized. The filter's spectrum is determined by the real and imaginary parts of the refractive index n and k (table in the appendix). They were recalculated

from the transmission for the pigment filters of 900 nm thickness as reported in Ref. [13]. The transmission profile of flat (no photon-trapping structure on the surface) and photon-trapping device is shown in Fig. 2. Such flat devices are studied here as a reference. Compared to the flat device (solid lines, Fig. 2), the devices with microhole structures (Fig. 3) exhibit higher transmission. The maximum possible optical efficiency for the blue, red, and green filters are determined by the filter transmission (FT) (Fig. 2, dashed lines) to be approx. $FT_{blue}= 80\%$ at 440 nm, $FT_{green} = 80\%$ at 550 nm, and $FT_{red} = 85\%$ at 650 nm, whereas the filters are almost transparent in the near-infrared. However, the absorption efficiency of Si is very weak in the near-infrared, where light trapping strategies are required to enhance the absorption by optical light trapping, bending, or slowing down the light. In this case, nano/micro holes are used to improve the absorption efficiency (Fig. 3).

III. RESULTS AND DISCUSSION

In the first part of the manuscript, finite difference time domain optical simulations were performed for the flat sensors. The simulated optical efficiency and transmittance after color filters (red, green, and blue) of the flat pixels are presented in Fig. 2. Dashed curves show the transmittance after the filters and the solid curves exhibit the optical efficiency in the pixels under the filter with the corresponding color. For this case, there is relatively low crosstalk for vertical illumination. As expected for silicon-based photodiodes, the optical efficiency in the infrared wavelengths is much lower than the optical efficiency for the visible
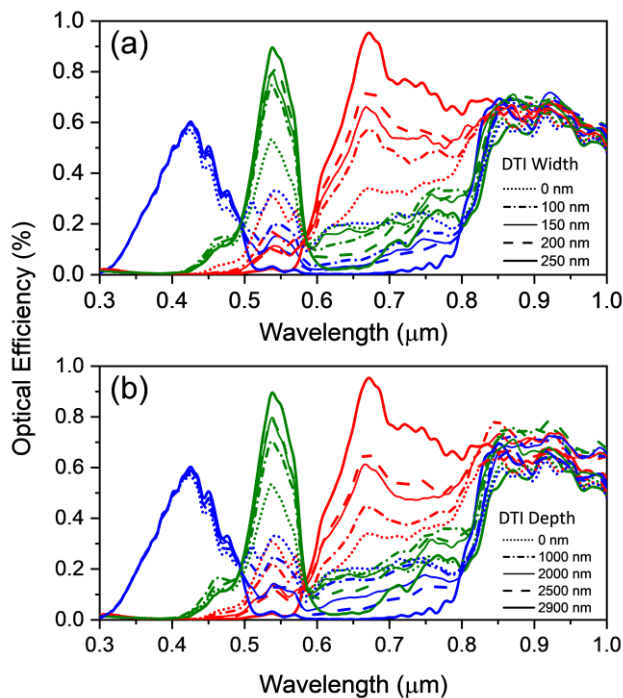

Fig. 4. Optimization of DTI (a) width and (b) depth in the CMOS image sensor. The influence of DTI width and depth was investigated in optical efficiency by varying them from 0 nm to 250 nm and 0 nm to 2900 nm, respectively.

wavelengths of blue, red, and green spectrum. The inherent indirect bandgap property of crystal silicon also leads to a high crosstalk in the infrared wavelength spectrum, resulting into high color error and poor color separation between blue-green and green-red [21].

However, the introduction of array of small inverted pyramids on the surface of an optical sensor can increase the optical efficiency as well as the crosstalk in the infrared wavelengths [8]. In this study, the influence of integrating such photon-trapping structures was investigated on the optical efficiency, while nano/microhole structures and their dimensions were varied. The investigated photon-trapping holey structures are: (a) inverted pyramids of 400×400 nm array [3], (b) cylindrical, (c) single inverted pyramid of 400×400 nm array, and (d) funnel shape. Furthermore, deep trench isolation was used between pixels to reduce the crosstalk. Silicon image sensors integrated with all the nanohole photon-trapping structures mentioned above were simulated for optical efficiency as presented in Fig. 3. Fig. 3 compares the simulated optical efficiency of the inverted pyramids of 400×400 nm array IR sensitivity enhancement of CMOS Image Sensor with diffractive light trapping pixels [3](a), cylindrical (b), single inverted pyramid of 900×900 nm (c), and funnel-shaped hole (d). The solid lines represent the pixel with trenches of 250 nm width and 2.5 μm deep, whereas the dashed lines show the pixels without trenches. While the hole arrays increase the optical efficiency up to about 40% at the near-infrared wavelengths, a single inverted pyramid hole of 900×900 nm can increase the optical efficiency to more than 60% at 850 nm wavelength. Moreover, an optimized single funnel-shaped holey photon-trapping structure can exhibit an optical efficiency up to 70%. The optical efficiencies of such image sensors calculated for a longer wavelength of 940 nm with encouraging results are also tabulated in Table I. For the wavelengths longer than 1.0 μm, the optical efficiency of the simulated image sensors sharply reduces and subsequently approaches to zero at 1.1 μm. Inverted pyramid and funnel shapes exhibit smaller reflection due to an effect that is similar to the Lambertian reflector. It helps trapping light in Si and better bending of the normal incident light into lateral modes, as was numerically and experimentally shown in [6]. While a guided resonant mode can be completely absorbed, high absorption can still be achieved with leaky modes that can propagate in the device long enough to be mostly absorbed. All the microstructures increased the absorption in the pixels for blue, green, and red with higher enhancement in the green and red wavelength spectrum.

Despite enhancing the optical efficiency, the integration of holes in the devices can increase the crosstalk between pixels. As mentioned, the crosstalk in the visible region is smaller than the near-infrared owing to the inherent material properties of the crystalline silicon. Hence, the color separation in the blue and green region is better than the red, expecting to be obtained a better color separation and low color error there [21]. However, the crosstalk can effectively be reduced by the implementation of trenches without any decrease in the optical efficiency. Table 1 shows the crosstalk

index of pixel which is a ratio between the intensity of that pixel to the intensity from the side pixel. Hence, the calculated higher crosstalk index indicates a better crosstalk value or lower crosstalk. The crosstalk was calculated for a pair of colors as tabulated on the pixel color column, where the intensity impact of one color pixel is calculated for the intensity from the another color pixel. On other words, crosstalk index of red-green pair indicates the intensity color pixel of red color for the intensity from the green pixel. Table 1 represents crosstalk index with and without trenches for all the shapes studied, while the crosstalk index presented for the flat pixels is used as a reference.   The flat pixels exhibit a very high crosstalk in red-green, green-blue, and blue-green, pronouncing crosstalk index of 4, 7.5, 2.97, respectively. However, the crosstalk was distinctly improved by introducing trenches between pixels as tabulated in Table 1. The trenches could be further optimized to provide the smallest crosstalk by varying their depths and thicknesses. In this study, the depth and width are the two degree of freedoms in the design of deep trench isolation for the optimization.

In the following, the influence of DTI width and the depth is studied on the optical efficiency and the crosstalk mainly in the near-infrared wavelengths as demonstrated in Fig. 4. In this case, a single funnel-shaped and tapered hole per pixel with a size comparable to the wavelength is used to maximize the optical efficiency of such image sensors. First, the width of the trench is varied ranging from 0 nm to 250 nm. The simulated CMOS image sensor exhibits a reduced crosstalk by increasing the width of the trench as shown in Fig. 4(a). In the next step, the depth of the trench is also varied from 0 nm to 2900 nm for the optical efficiency of the sensors as depicted in Fig. 4(b), suggesting that the crosstalk can be decreased with the increase of the trench depth. However, such image sensor can be optimized with a reasonable crosstalk for the trench depth and width of 2500 nm and 150 nm, respectively. The crosstalk for a blue pixel from a red pixel is defined as a ratio between the response of the blue pixel near the 440 nm wavelength in the range +/- 10 nm to the response of the red pixel for the same wavelength range. In the case of near-infrared wavelengths, there will be an equal response from all three pixels and will be represented as a grayscale picture. The simulations show that while the crosstalk decreased, the optical efficiency is increased for all the colors due to the use of single holes with trenches.

Single microhole per pixel image sensors studied here with enhanced absorption efficiency in the near infrared can be fabricated by standard CMOS compatible processes. We fabricated several photon trapping photodetectors integrated with microhole structures, including funnel-shaped, cylindrical, and inverted pyramid using wet or dry etching [5]. So far, we have not fabricated an actual CMOS image sensor with such microhole structures per-pixel. However, Sony used anisotropic wet etching on 100 silicon to form inverted pyramid arrays [2] , and Samsung utilized dry etched shallow trenches (backside scatter technology) to fabricate image sensors [1]. In this case, we can either wet etch a large single inverted pyramid or dry etch a cylindrical or funnel hole [5]. The single holes can be filled with SiO_2 and planarized for subsequent processing.

IV. Conclusion

We presented silicon CMOS sensors with backside-illumination designed using 3 μm thick silicon and with 1.12 μm × 1.12 μm pixel size in RGB. Optical simulations were conducted using FDTD methods. We have shown that a single hole with a size of about 900 nm increases the optical efficiency of the image sensors for all the colors and in near-infrared wavelengths. In the near-infrared wavelengths, the optical efficiency of the sensors could be as high as 70% by implementing such optimized holey photon-trapping microstructure. Our simulation shows that the lateral modes are responsible for the enhanced absorption. The hole shapes were investigated and optimized based on the modal analysis. We have shown that funnel and tapered holes with a size comparable with the wavelength exhibit the highest optical efficiency. The crosstalk increased due to the use of holes, but it was reduced back to normal level with the implementation of trenches between individual pixels. We optimized trenches with 150 nm width and 2.5 μm depth for minimum crosstalk.

Acknowledgment

Appendix

The complex optical constants ($n+ik$) of color filters, where the real part of the optical constants is called refractive index (n) and imaginary part is called extinction coefficient (k), was used in the optical simulation of the image sensors. The data was taken from [10][11]. Table II represents the parameters of the filters which were used in the simulations.

References

[1]   C. F. Han, J. M. Chiou, and J. F. Lin, "Deep trench isolation and inverted pyramid array structures used to enhance optical efficiency of photodiode in CMOS image sensor via simulations," *Sensors (Switzerland)*, 2020, doi: 10.3390/s20113062.

[2]   I. Oshiyama *et al.*, "Near-infrared sensitivity enhancement of a back-illuminated complementary metal oxide semiconductor image sensor with a

TABLE II : Filters parameters [10-11]

Wavelength, nm	blue n	k	Green n	k	Red n	k
300	1.55	0.055	1.62	0.4	1.54	0.415
400	1.54	0.07	1.6	0.5	1.54	0.325
500	1.54	0.215	1.58	0.405	1.53	0.155
600	1.54	0.8	1.57	0.05	1.53	0.048
700	1.53	0.45	1.57	0.11	1.52	0.033
800	1.53	0.455	1.57	0.105	1.52	0.375
900	1.52	0.465	1.56	0.09	1.52	0.0185
1000	1.52	0.39	1.56	0.055	1.52	0.015

pyramid surface for diffraction structure," in *Technical Digest - International Electron Devices Meeting, IEDM*, 2018, doi: 10.1109/IEDM.2017.8268403.

[3] S. Yokogawa *et al.*, "IR sensitivity enhancement of CMOS Image Sensor with diffractive light trapping pixels," *Sci. Rep.*, 2017, doi: 10.1038/s41598-017-04200-y.

[4] R. Fontaine, "The State-of-the-Art of Smartphone Imagers," *Proc. Int. Image Sens. Work.*, 2019.

[5] Y. Gao *et al.*, "Photon-trapping microstructures enable high-speed high-efficiency silicon photodiodes," *Nat. Photonics*, 2017, doi: 10.1038/nphoton.2017.37.

[6] Y. Gao *et al.*, "High Speed Surface Illuminated Si Photodiode Using Microstructured Holes for Absorption Enhancements at 900-1000 nm Wavelength," *ACS Photonics*, 2017, doi: 10.1021/acsphotonics.7b00486.

[7] J. Ahn *et al.*, "Advanced image sensor technology for pixel scaling down toward l.Oμm (Invited)," in *Technical Digest - International Electron Devices Meeting, IEDM*, 2008, doi: 10.1109/IEDM.2008.4796671.

[8] B. J. Park *et al.*, "Deep trench isolation for crosstalk suppression in active pixel sensors with 1.7 μm pixel pitch," *Japanese J. Appl. Physics, Part 1 Regul. Pap. Short Notes Rev. Pap.*, 2007, doi: 10.1143/JJAP.46.2454.

[9] A. Tournier *et al.*, "Pixel-to-Pixel isolation by Deep Trench technology : Application to CMOS Image Sensor," *Proc. 2011 Int. Image Sens. Work.*, 2011.

[10] "Imaging and Sensing Technology │ Imaging and Sensing Technology │ Sony Semiconductor Solutions Group." https://www.sony-semicon.co.jp/e/technology/imaging-sensing/ (accessed Nov. 22, 2020).

[11] S. Yokogawa, S. P. Burgos, and H. A. Atwater, "Plasmonic color filters for CMOS image sensor applications," *Nano Lett.*, 2012, doi: 10.1021/nl302110z.

[12] Y. Horie *et al.*, "Visible Wavelength Color Filters Using Dielectric Subwavelength Gratings for Backside-Illuminated CMOS Image Sensor Technologies," *Nano Lett.*, 2017, doi: 10.1021/acs.nanolett.7b00636.

[13] C. Park and M. G. Kang, "Color restoration of RGBN multispectral filter array sensor images based on spectral decomposition," *Sensors (Switzerland)*, 2016, doi: 10.3390/s16050719.

[14] D. Hertel, H. Marechal, D. A. Tefera, W. Fan, and R. Hicks, "A low-cost VIS-NIR true color night vision video system based on a wide dynamic range CMOS imager," in *IEEE Intelligent Vehicles Symposium, Proceedings*, 2009, doi: 10.1109/IVS.2009.5164290.

[15] B. E. Bayer, "Color Imaging Array," 1976.

[16] H. Cansizoglu *et al.*, "A New Paradigm in High-Speed and High-Efficiency Silicon Photodiodes for Communication-Part I: Enhancing Photon-Material Interactions via Low-Dimensional Structures," *IEEE Trans. Electron Devices*, 2018, doi: 10.1109/TED.2017.2779145.

[17] H. Cansizoglu *et al.*, "A New Paradigm in High-Speed and High-Efficiency Silicon Photodiodes for Communication-Part II: Device and VLSI Integration Challenges for Low-Dimensional Structures," *IEEE Transactions on Electron Devices*. 2018, doi: 10.1109/TED.2017.2779500.

[18] S. Ghandiparsi *et al.*, "High-Speed High-Efficiency Photon-Trapping Broadband Silicon PIN Photodiodes for Short-Reach Optical Interconnects in Data Centers," *J. Light. Technol.*, 2019, doi: 10.1109/JLT.2019.2937906.

[19] A. Taflove, S. C. Hagness, and M. Piket-May, "Computational Electromagnetics: The Finite-Difference Time-Domain Method," in *The Electrical Engineering Handbook*, 2005.

[20] "High-Performance Photonic Simulation Software - Lumerical." https://www.lumerical.com/ (accessed Nov. 22, 2020).

[21] M. I. Hossain *et al.*, "Perovskite Color Detectors: Approaching the Efficiency Limit," *ACS Appl. Mater. Interfaces*, 2020, doi: 10.1021/acsami.0c12851.

Ekaterina Ponizovskaya Devine received the M.S. and Ph.D. degrees from the Moscow Institute of Physics and Technology (State University), Moscow, Russia, in 1999.

She was with the Ames Center, NASA, Mountain View, CA, USA, where she was involved in the optimization and physics-based models for prognostics and automation. She is currently with W&WSens Device, Inc., Los Altos, CA, USA, where she is focusing on photonics and photodetectors.

Wayesh Qarony received his B.Sc. degree in Electrical & Electronic Engineering from American International University-Bangladesh (AIUB) in 2010, M.Sc. degree in Electrical Engineering from Jacobs University Bremen, Germany in 2013, and Ph.D. in Applied Physics from The Hong Kong Polytechnic University in 2019. He also studied M.Sc. in Telecommunication Engineering from University of Trento, Italy.

He was a lecturer and then senior lecturer in Electrical & Electronic Engineering at AIUB. He is currently with University of California, Davis, CA, USA as a Postdoctoral Scholar in Electrical and Computer Engineering. He is interested in multispectral image sensor, nanophotonic design and fabrication of solar cells and photosensors.

Ahmed S. (Surrati) Mayet received the B.Sc. degree in physics from Taibah University, Medina, Saudi Arabia, and the master's degree in electrical and computer engineering from the University of California, Davis, CA, USA, in 2017, where he is currently pursuing the Ph.D. degree with the Electrical and Computer Engineering Department. His research focuses on the development of high-speed and high-efficiency photodetectors for optical communication systems.

Ahasan Ahamed is a second-year graduate student pursuing his Ph.D. degree in the Electrical and Electronics Engineering Department at the University of California, Davis. He received a B. Sc. Degree from Bangladesh University of Engineering and Technology in 2018. He is currently working on spectral response engineering of photon-trapping photodiodes paving towards spectrometer-on-a-chip. His research works also include designing ultra-fast photodiodes and SPADs for hyperspectral imaging.

Soroush Ghandiparsi received the B.Sc. degree in electrical engineering and the M.Sc. degree in nanophotonic engineering from the School of Engineering Emerging Technology, Sharif University of Technology, Tehran, Iran, in 2009 and 2012, respectively. He received Ph.D. in electrical engineering with emphasis in Biophotonics and Bioimaging from the University of California-Davis. His research has been involved in developing high-speed and efficient optoelectronic devices for high-speed communication, biomedical imaging, and NIR imaging and sensing. Currently, he is a post-doctoral scholar at department of Biomedical Engineering, UCDavis, working on interferometric NIR spectroscopy for tissue flowmetery and Oximetery

Cesar Bartolo-Perez received the B.Sc. in Technology from the National Autonomous University of Mexico in 2012, and the M.Sc. in Electrical Engineering from the National Institute for Astrophysics Optics and Electronics, Mexico, in 2015. He is currently pursuing the Ph.D. degree in Electrical and Computer Engineering at University of California, Davis, CA, USA. His current research focused on Single Photon Avalanche Photodetectors for Imaging and Sensing.

Toshishige Yamada (SM'11) received the B.S. and M.S. degrees in physics from the University of Tokyo, Tokyo, Japan, and the Ph.D. degree in electrical engineering from Arizona State University, Tempe, AZ, USA.

He joined the NASA Ames Research Center, Moffett Field, CA, USA. He is currently with the University of California at Santa Cruz, Santa Cruz, CA, USA, and is involved in the studies of advanced materials and devices.

Aly F. Elrefaie (M'83–SM'86–F'04–LF'19) received the B.S.E.E. degree (Hons.) from Ain Shams University, Cairo, Egypt, in 1976, and the M.Sc. and Ph.D. degrees in electrical engineering from NYU, Brooklyn, NY, USA, in 1980 and 1983, respectively.

Since 2014, he has been a Chief Scientist with W&Wsens Devices, Inc., Los Altos, CA, USA, where he is focusing on topics related to nano technology in optical communications

Shih-Yuan (SY) Wang (LF'12) B.S. Engineering Physics 1969, UC Berkeley; Ph.D. Electrical Engineering and Computer Sciences, 1977 UC Berkeley. At HP Labs, SY worked on multimode vertical cavity surface emitting lasers and high speed III-V photodiodes, both of which became successful products. SY is currently with, W&WSens Devices, Inc. Los Altos, CA, working on silicon photodiodes compatible with CMOS process for CMOS image sensors, optical interconnects and LiDAR applications.

M. Saif Islam (M'98–SM'15–F'20) received the B.Sc. degree in physics from Middle East Technical University, Ankara, Turkey, in 1994, the M.S. degree in physics from Bilkent University, Ankara, in 1996, the MS and the Ph.D. degree in electrical engineering from UCLA, Los Angeles, CA, USA, in 1999 and 2001 respectively. He worked for JDS Uniphase and HP Labs before joining UC Davis in 2004 where he is a Professor of Electrical and Computer Engineering now.